Supporting material for

Strengthening polylactic acid (PLA) composites with poly(methyl methacrylate)-functionalized cellulose nanofibrils created through grafting-through emulsion polymerization

Hathaithep Senkum,[1,2] Peter V. Kelly,[1,2] Ahmad A. L. Ahmad,[1,2] Siamak Shams Es-haghi,[2,3] William M. Gramlich[1,2,4,*]

[1]**Department of Chemistry, University of Maine, Orono, ME, 04469, USA**

[2]**Advanced Structures and Composites Center, University of Maine, Orono, ME 04469, USA**

[3]**Department of Chemical and Biomedical Engineering, University of Maine, Orono, ME, 04469, USA**

[4]**Forest Bioproducts Research Institute, University of Maine, Orono, ME, 04469, USA**

[*]**Corresponding author: william.gramlich@maine.edu**

Table S1. Weight percent of PMMA on the cellulose surfaces before and after DCM purification

Material	Molar ratios of MMA:cellobiose:KPS	%wt PMMA (before DCM purification)	%wt PMMA (after DCM purification)
PMMA-MetCNF	50:1:0.06	39 ± 6	32 ± 5
PMMA-MetCNF	50:1:0.12	41 ± 6	32 ± 5

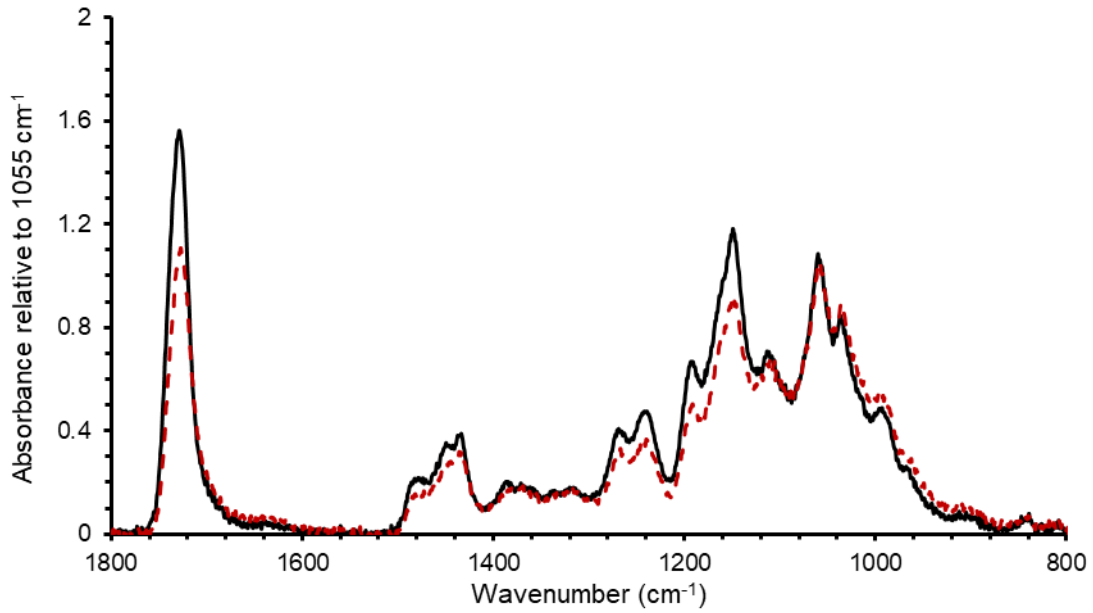

Figure S1. ATR-IR spectra of PMMA-MetCNFs (50:1:0.06) before (black solid line) and after DCM purification to remove non-covalently bound PMMA (red dashed line) normalized to the C-O stretching band of the cellulose at 1055 cm^{-1}.

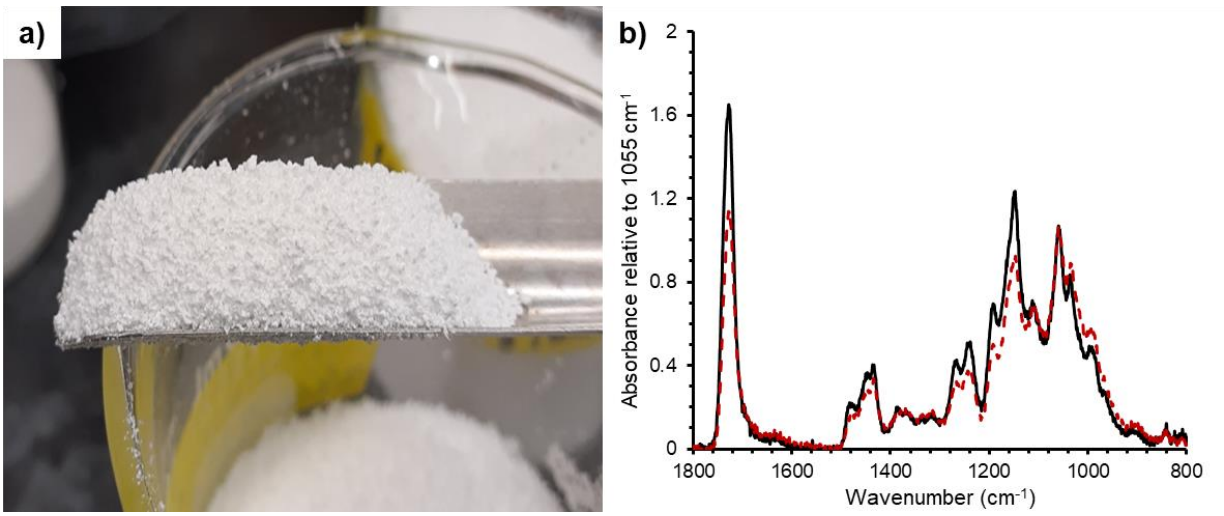

Figure S2. (A) Ground PMMA-MetCNFs (50:1:0.12) after vacuum-drying and grinding. B) ATR-IR spectra of PMMA-MetCNFs (50:1:0.12) before (black solid line) and after DCM purification to remove non-covalently bound PMMA (red dashed line) normalized to the C-O stretching band of the cellulose at 1055 cm^{-1}.

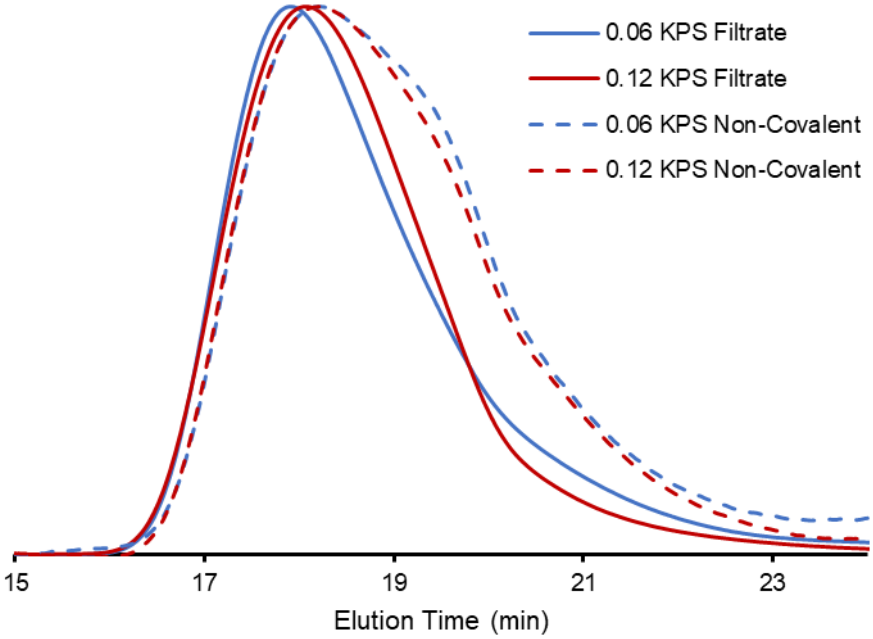

Figure S3. SEC elution curves of the PMMA filtrate (solid lines) and the non-covalently bound PMMA (dashed lines) for 50:1:0.06 (red lines) and 50:1:0.12 (blue lines) molar ratio conditions.

Table S2. SEC data for peak molecular weight (M_p), number average molecular weight (M_n), and dispersity ($Đ$) for the PMMA filtrate particles (SFEP particles) and noncovalently bound polymer extracted from the PMMA-MetCNFs synthesized at the MMA:cellobiose:KPS molar ratios given as reaction conditions.

Reaction Conditions	*Collected Polymer*	$M_p\ (kg/mol)$	$M_n\ (kg/mol)$	$Đ$
50:1:0.06	Filtrate	903	126	5.94
50:1:0.06	Non-covalent	692	150	3.72
50:1:0.12	Filtrate	790	211	3.64
50:1:0.12	Non-covalent	697	143	4.10

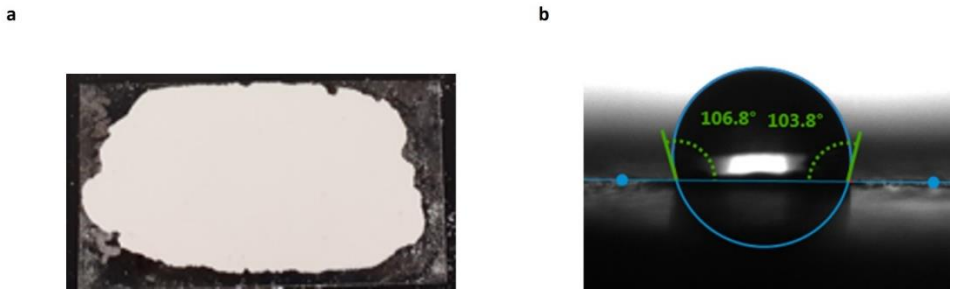

Figure S4. (A) Representative specimen of the ground PMMA-MetCNFs (50:1:0.06) that was compressed on a glass slide at 500 psi for 5 minutes under ambient temperature for static water contact angle measurement. (B) Representative static water contact angle droplet on PMMA-MetCNFs (50:1:0.06) surface at 15 seconds.

Table S3. Measured dispersive (γ^d), polar (γ^{sp}), acceptor (γ^+), donor (γ^-), and total (γ) surface energy components for PMMA-MetCNFs and PLA.

	50:1:0.06				
n/n_0	γ^d (mJ/m^2)	γ^{sp} (mJ/m^2)	γ^- (mJ/m^2)	γ^+ (mJ/m^2)	γ (mJ/m^2)
0.01	47.2	12.7	11.0	3.6	59.8
0.02	40.9	12.1	10.2	3.6	53.0
0.03	35.8	11.0	9.2	3.3	46.8
0.05	33.8	10.7	9.3	3.1	44.5
0.10	25.5	8.6	7.7	2.4	34.1
	50:1:0.12				
n/n_0	γ^d (mJ/m^2)	γ^{sp} (mJ/m^2)	γ^- (mJ/m^2)	γ^+ (mJ/m^2)	γ (mJ/m^2)
0.01	44.5	12.3	10.7	3.5	56.8
0.02	40.7	11.5	10.5	3.2	52.3
0.03	37.5	10.8	9.9	2.9	48.3
0.05	37.5	11.0	10.3	2.9	48.5
0.10	33.8	10.9	10.1	3.0	44.7
	PLA				
n/n_0	γ^d (mJ/m^2)	γ^{sp} (mJ/m^2)	γ^- (mJ/m^2)	γ^+ (mJ/m^2)	γ (mJ/m^2)
0.01	122.9	35.6	53.9	5.9	158.5
0.02	75.2	22.8	32.0	4.1	97.9
0.03	67.8	19.0	29.3	3.1	86.8
0.05	62.1	17.4	27.0	2.8	79.5
0.10	55.9	15.6	24.2	2.5	71.5

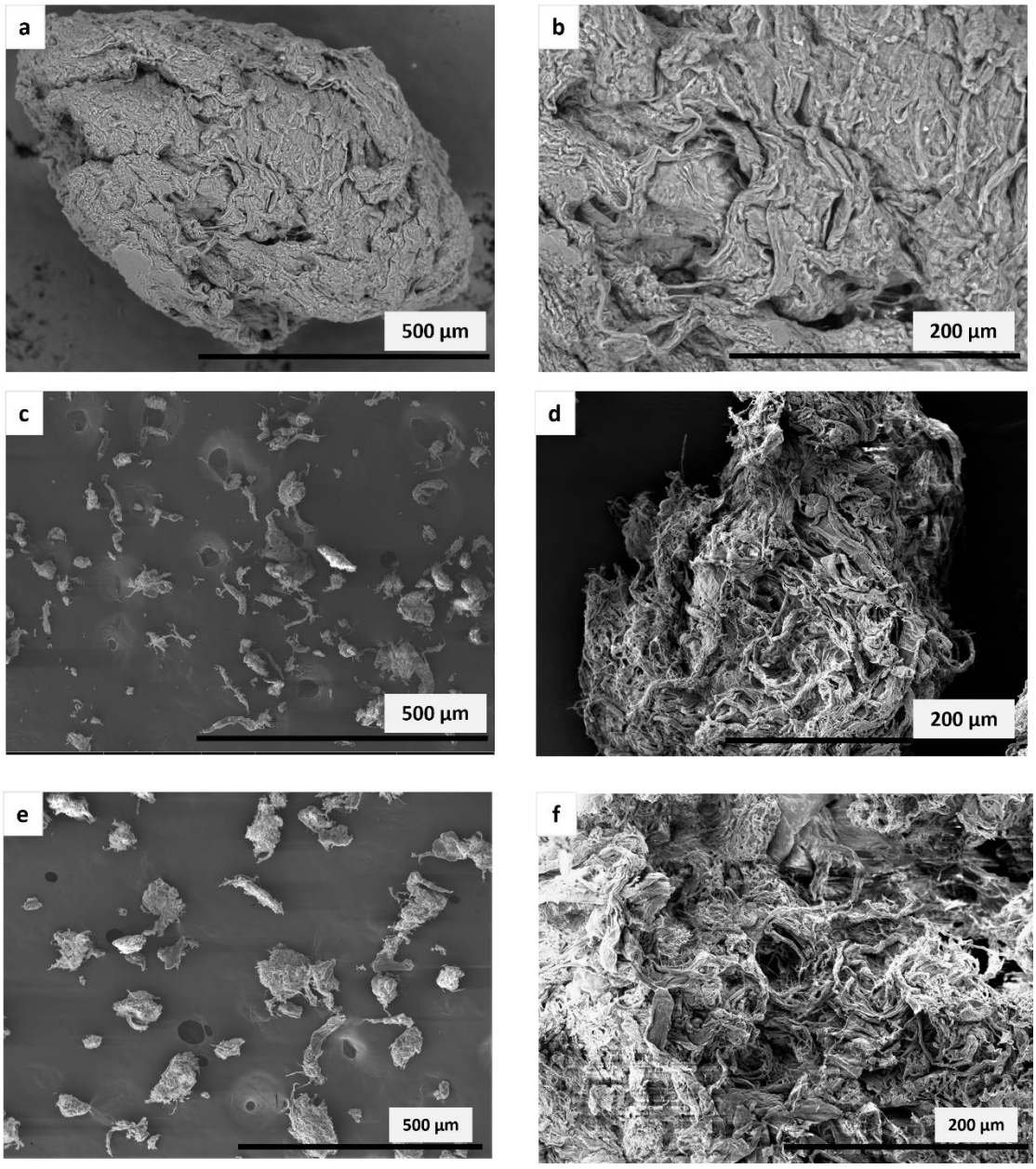

Figure S5. Representative SEM images of the (a and b) unmodified CNFs, (c and d) PMMA-MetCNFs (50:1:0.06), and (e and f) PMMA-MetCNFs (50:1:0.12) after drying and grinding at 200x magnification (left images) and at 500x magnification (right images).

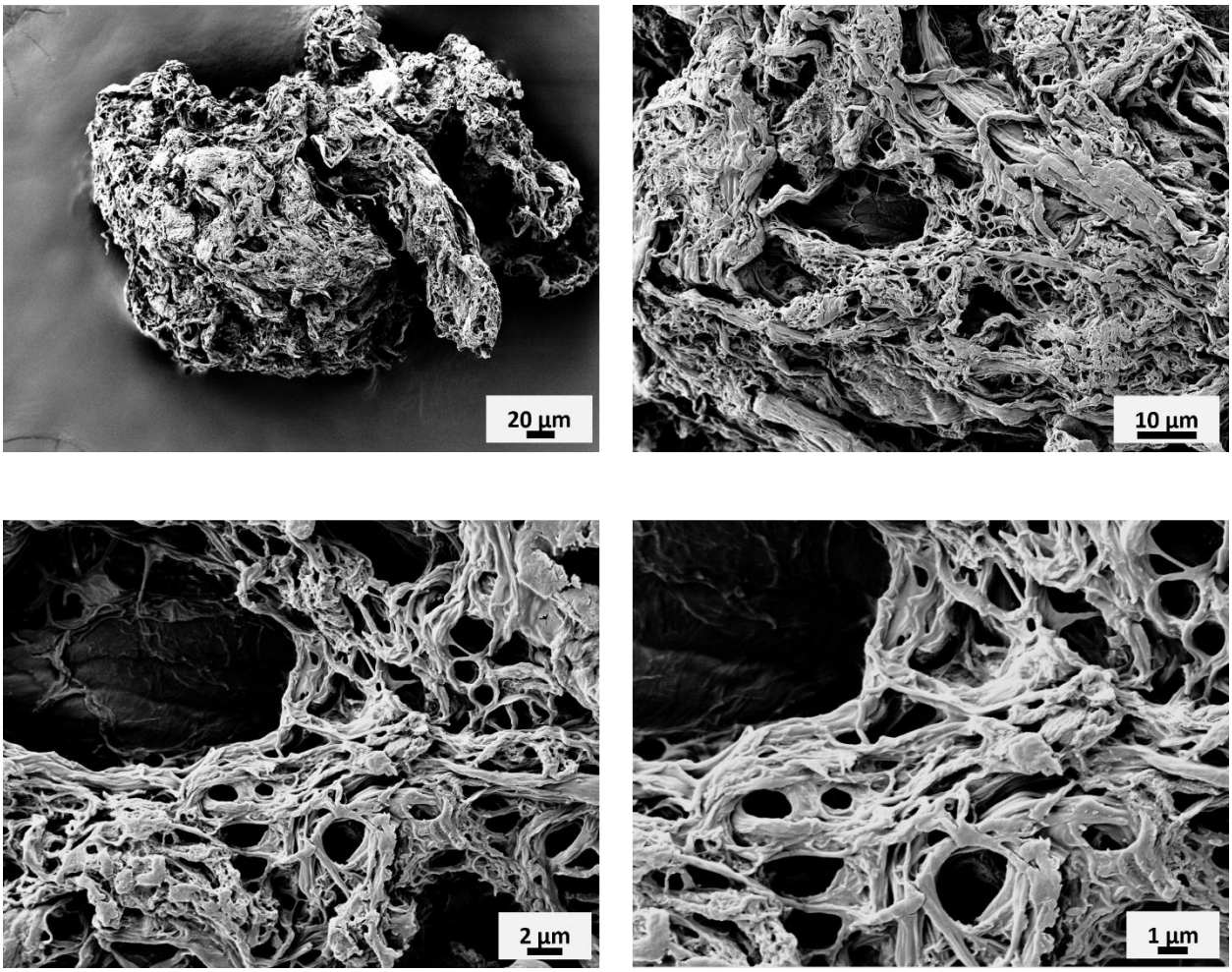

Figure S6. Representative SEM images of PMMA-MetCNFs (50:1:0.06) after removing the non-covalently bound PMMA with DCM and drying in a vacuum oven at 40 °C.

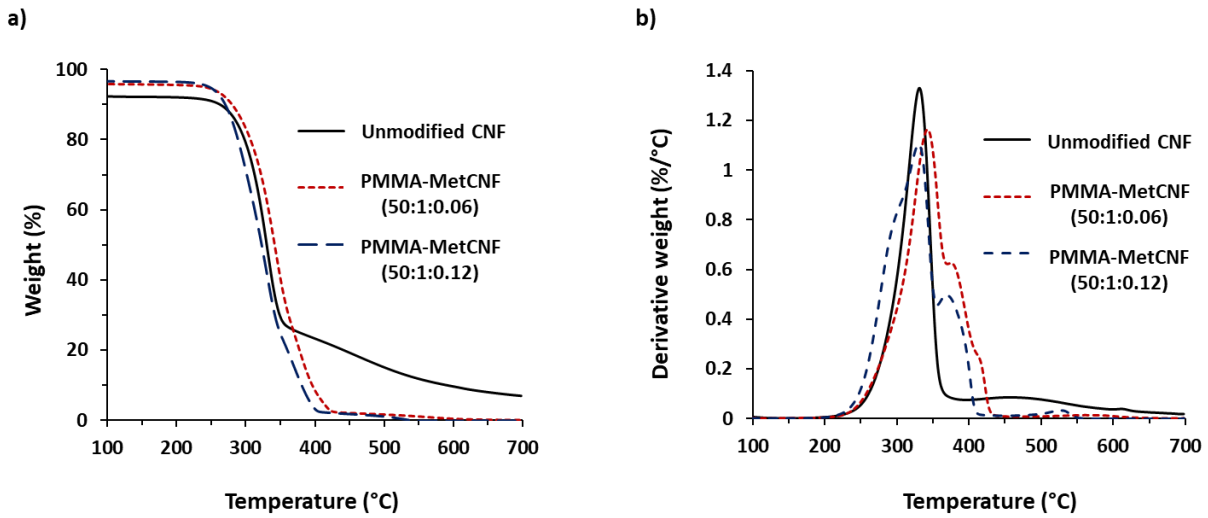

Figure S7. TGA (a) weight loss and (b) derivative weight loss curves of the spray-dried unmodified CNFs and the ground PMMA-MetCNFs without extraction with DCM.

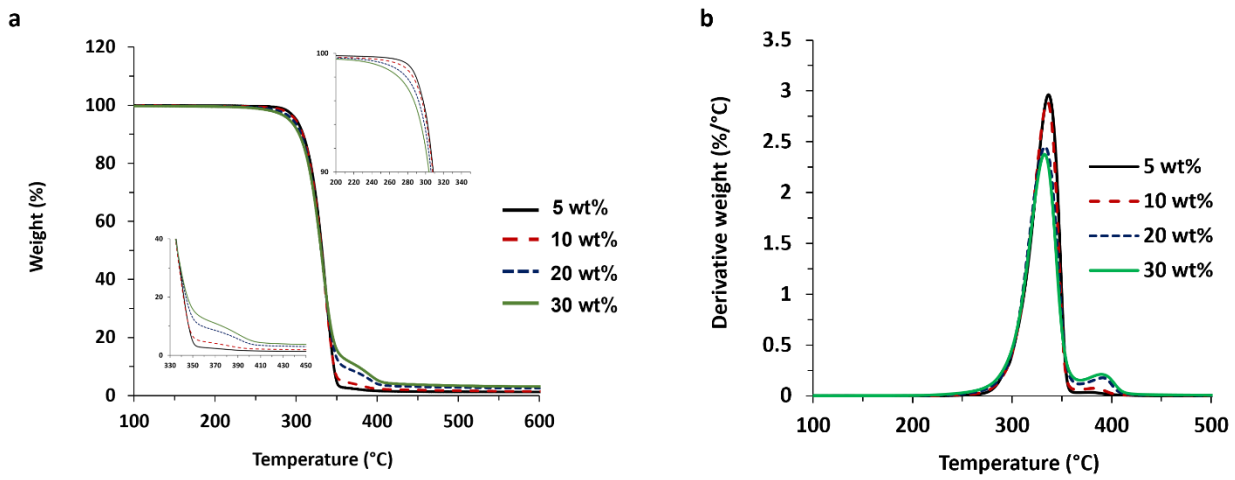

Figure S8. TGA (a) weight loss and (b) derivative weight loss curves of PLA composites reinforced by PMMA-MetCNFs (50:1:0.06).

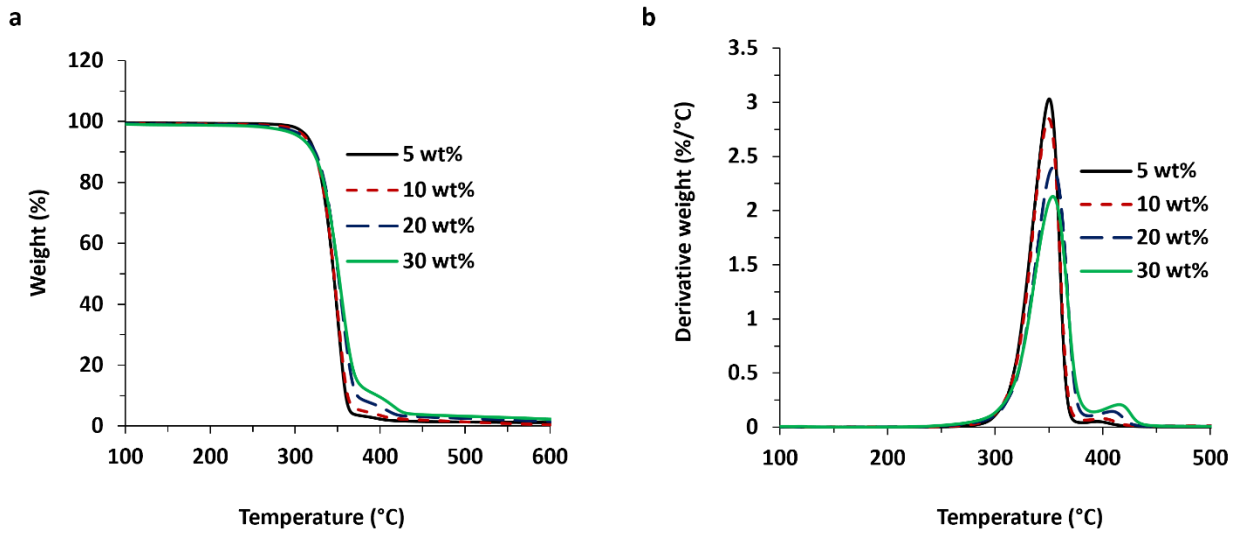

Figure S9. TGA (a) weight loss and (b) derivative weight loss curves of PLA composites reinforced by PMMA-MetCNFs (50:1:0.12).

Table S4. Mechanical properties of neat PLA and PLA composites containing PMMA-MetCNFs with different reinforcement loadings.

Composite sample	Reinforcement content (wt%)	Tensile Strength (MPa)	Tensile Modulus (GPa)	% Tensile strength improvement	% Tensile modulus improvement
Neat PLA	0	62 ± 3	3.2 ± 0.1	0	0
PMMA-MetCNF (50:1:0.06)	5	62 ± 4	3.7 ± 0.2	-1	13
PMMA-MetCNF (50:1:0.06)	10	64 ± 4	3.9 ± 0.1	3	19
PMMA-MetCNF (50:1:0.06)	20	79 ± 3	4.5 ± 0.1	27	39
PMMA-MetCNF (50:1:0.06)	30	78 ± 5	5.0 ± 0.2	26	55
PMMA-MetCNF (50:1:0.12)	5	68 ± 2	3.7 ± 0.2	9	13
PMMA-MetCNF (50:1:0.12)	10	69 ± 3	3.9 ± 0.1	10	19
PMMA-MetCNF (50:1:0.12)	20	68 ± 3	4.2 ± 0.1	9	31
PMMA-MetCNF (50:1:0.12)	30	59 ± 7	4.4 ± 0.3	-6	34

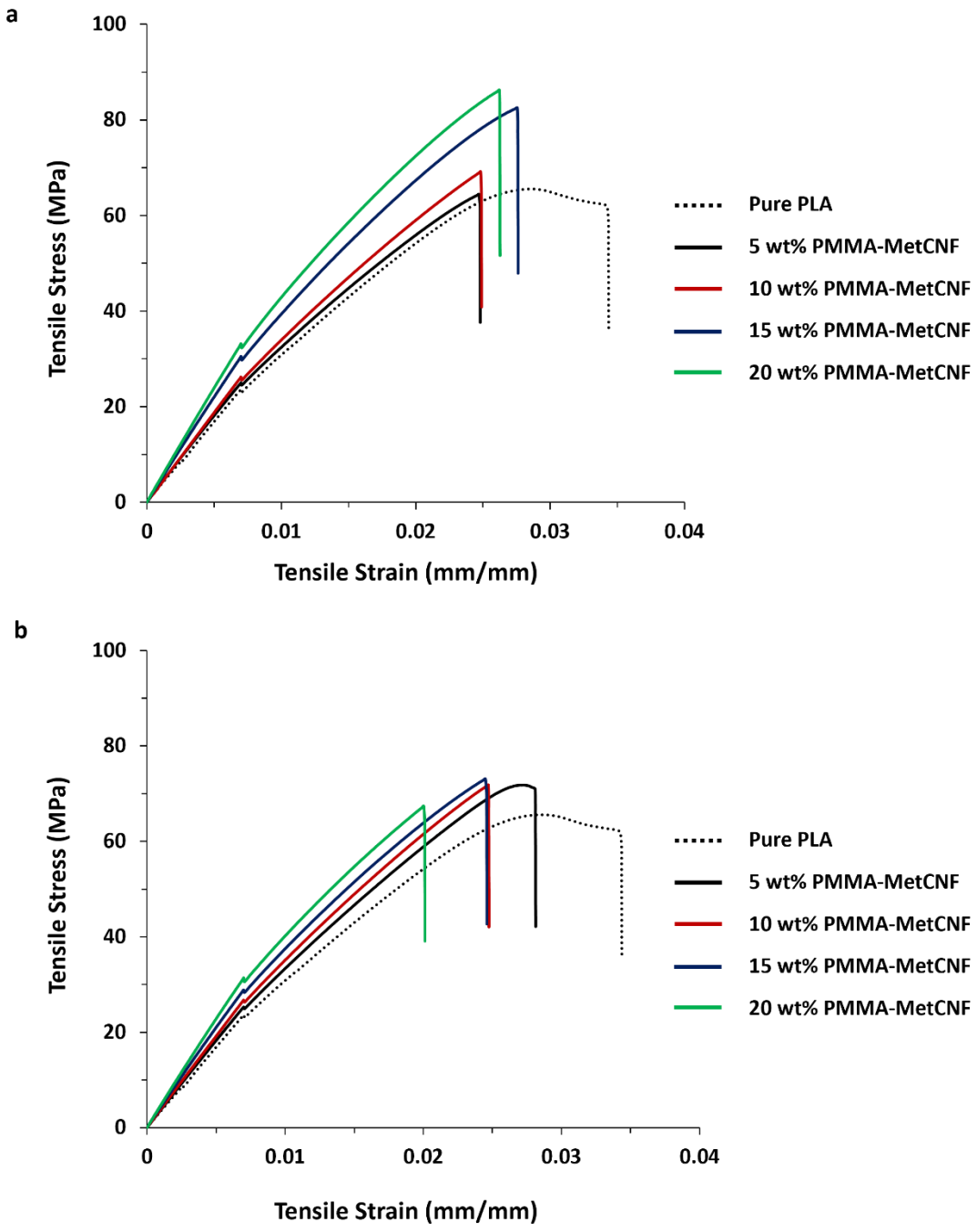

Figure S10. Representative stress-strain curves of pure PLA and PMMA-MetCNF composites for (A) PMMA-MetCNFs (50:1:0.06) and (B) PMMA-MetCNFs (50:1:0.12). The small dip below 0.01 mm/mm resulted from the removal of the extensometer at 0.007 mm/mm.

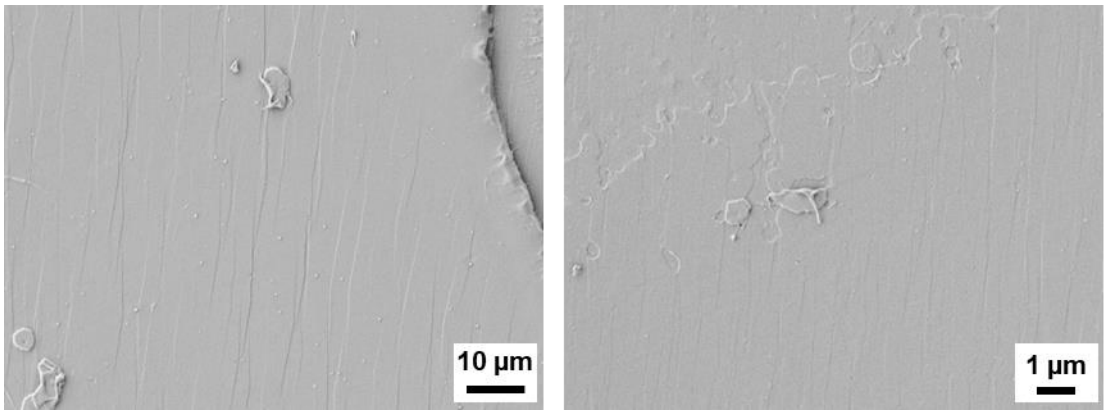

Figure S11. Representative SEM images of PLA fracture surfaces at 1000x (left) and 7000x (right) magnification.

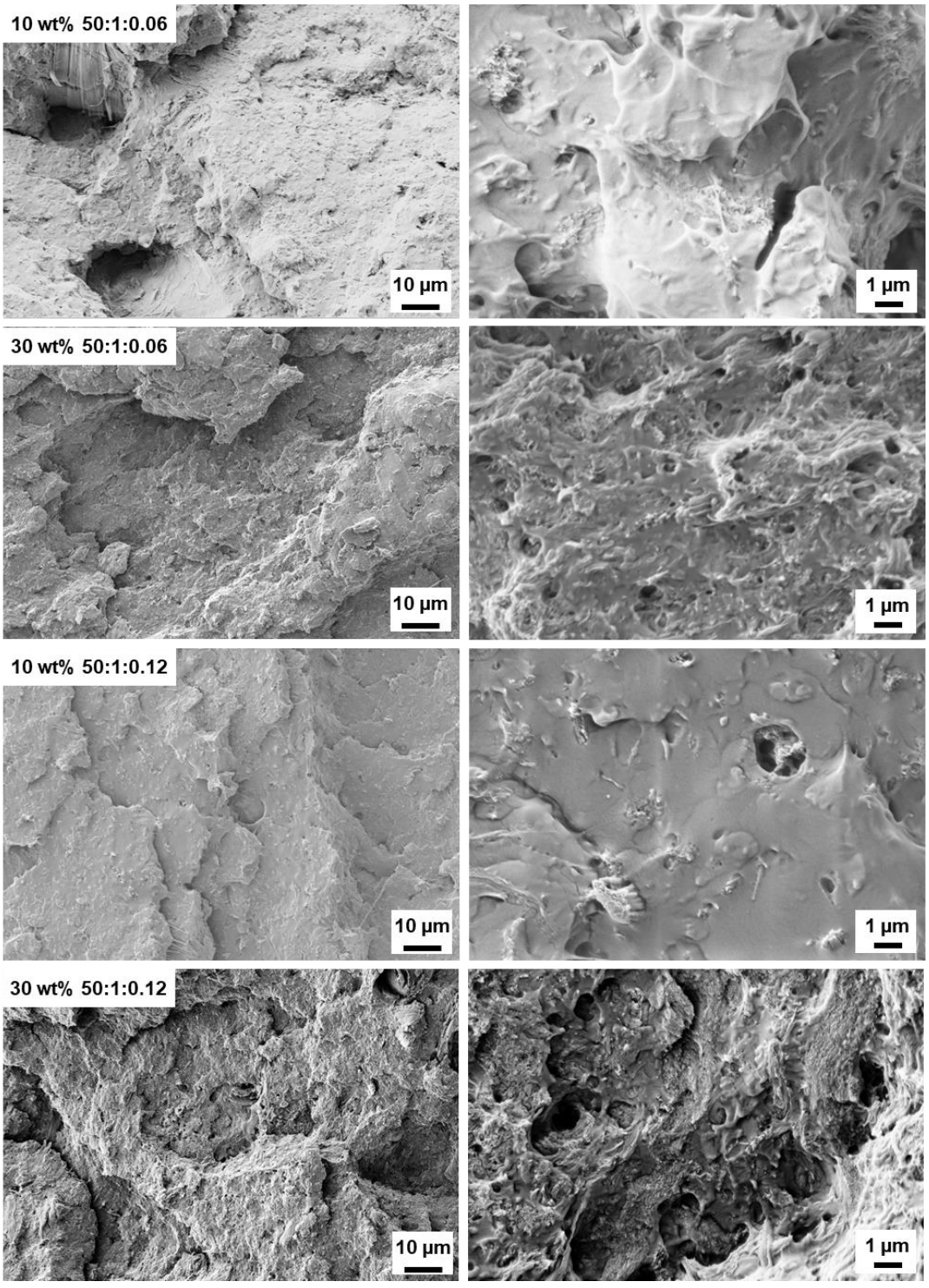

Figure S12. Representative SEM images of tensile bar fracture surfaces of the PMMA-CNF composites with 10 wt% and 30 wt% PMMA-MetCNF reinforcements at 1000x (left images) and 7000x magnification (right images).

Table S5. The thermal properties of pure PLA and PLA composites derived from DSC analysis.

Sample	Wt% fibers	T_g[a] (°C)	T_{cc}[a] (°C)	T_m[a] (°C)	ΔH_c[b] (J/g)	ΔH_m[b] (J/g)	X_c (%)
Neat PLA	0	54.4	117.0	151.8	25.7	28.3	2.8
PMMA-MetCNF (50:1:0.06)	5	56.0	105.4	145.4	22.7	23.0	0.3
PMMA-MetCNF (50:1:0.06)	10	56.2	106.6	145.8	19.2	21.4	2.6
PMMA-MetCNF (50:1:0.06)	20	56.4	114.1	147.1	15.6	16.8	1.6
PMMA-MetCNF (50:1:0.06)	30	56.3	124.5	150.1	4.7	5.3	0.9
PMMA-MetCNF (50:1:0.12)	5	55.4	106.7	147.7	23.6	24.4	0.9
PMMA-MetCNF (50:1:0.12)	10	55.6	106.6	145.7	21.5	21.7	0.2
PMMA-MetCNF (50:1:0.12)	20	55.9	114.0	147.6	16.5	17.3	1.1
PMMA-MetCNF (50:1:0.12)	30	56.0	125.2	150.2	1.7	2.0	0.5

[a]Obtained from the second heating cycle. [b]Measured from the first heating cycle. The thermal data of the glass transition temperature (T_g), cold crystallization temperature (T_{cc}), and melting temperature (T_m) were measured from the second heating cycle. The enthalpies of cold crystallization (ΔH_c) and enthalpies of melting (ΔH_m) were generated from the first heating cycle. The degree of crystallization (X_c) was calculated as described in the methods.